Published in final edited form as:
J Am Soc Mass Spectrom. 2009 April ; 20(4): 682–688. doi:10.1016/j.jasms.2008.12.004.

Selection of the Optimum Electrospray Voltage for Gradient Elution LC-MS Measurements

Ioan Marginean, **Ryan T. Kelly**, **Ronald J. Moore**, **David C. Prior**, **Brian L. LaMarche**, **Keqi Tang**, and **Richard D. Smith***
Biological Sciences Division, Pacific Northwest National Laboratory, P.O. Box 999, Richland, Washington 99352

Abstract

Changes in liquid composition during gradient elution liquid chromatography (LC) coupled to mass spectrometry (MS) analyses affect the electrospray operation. To establish methodologies for judicious selection of the electrospray voltage, we monitored in real-time the effect of the LC gradient on the spray current. The optimum range of the electrospray voltage decreased as the concentration of organic solvent in the eluent increased during reversed-phase LC analyses. These results provided the means to rationally select the voltage so as to ensure effective electrospray operation throughout gradient-elution LC separations. For analyses in which the electrospray was operated at constant voltage, a small run-to-run variation in the spray current was observed, indicating a changing electric field due to fouling or degradation of the emitter. Algorithms using feedback from spray current measurements to maintain the electrospray voltage within the optimum operating range throughout gradient elution LC-MS were evaluated. The electrospray operation with voltage regulation and at a constant, judiciously selected voltage during gradient elution LC-MS measurements produced data with similar reproducibility.

SYNOPSIS—Electrospray current measurements during gradient elution liquid chromatography analyses provide reliable feedback for monitoring, understanding, and improving performance.

INTRODUCTION

Electrospray ionization (ESI) has enabled the successful on-line coupling of liquid chromatography (LC) with mass spectrometry (MS),[1,2] a combination that has become the de facto standard for proteomics research.[3,4] Despite the tremendous technological growth of LC-MS, the electrospray remains a seemingly robust but relatively neglected and poorly understood intermediate. It is expected that shifting eluent composition during gradient LC analyses may alter the electrospray operation; however, essentially all gradient elution LC-MS analyses are performed with little or no feedback with respect to electrospray performance.

During LC-MS analyses, the solvent composition and flow rate are dictated by the separation conditions and only the applied voltage and the emitter-MS inlet distance can be adjusted. Direct optimization of the analyte signal prior to data acquisition is not possible, as for infusion measurements. The voltage is usually selected according to the instrument manufacturer recommendations or previous experience, rather than careful consideration of the experimental conditions. Adjusting the emitter-MS inlet distance induces large changes in the electric field driving the electrospray due to the nonlinear dependence between the two parameters. This may result in different electrospray current or even a different operating regime.[5] When non-metallic (e.g. fused silica) emitters are used, the voltage is usually applied upstream of the

*Corresponding author. Email: rds@pnl.gov

emitter via a conductive material in contact with the solution. The voltage drop across the emitter should also be considered in this case;[6] applying the same voltage on emitters of different lengths positioned at the same distance in front of the MS inlet would also result in different electric fields.

The voltage that ensures optimum operation at the beginning of the analysis may not be appropriate for the solvent mixture eluting at the end of the gradient. The electrospray characteristic curves measured with several solvent compositions simulating a typical reversed-phase liquid chromatography (RPLC) gradient indicated that the voltage required to maintain the electrospray in a specific operating regime decreases significantly with increasing organic solvent concentration.[5] The vast majority of LC-MS analyses are currently performed with constant electrospray voltage; previous experience with a specific type of analysis may help guiding the selection of a reasonable voltage for the beginning of the gradient that is not too high or too low for the end of the gradient. The changing eluent composition can be counterbalanced by post-column combination with an inverted gradient;[7] this approach provides steady solvent composition throughout the analysis at the cost of decreased sensitivity due to the increased flow rate and analyte dilution.

Only a few attempts to rationally control the electrospray operation during LC-MS analyses have been described. Valaskovic et al. used feedback from an electrospray imaging system to automatically adjust the applied voltage and control its operating regime.[8] Two recently reported techniques aimed at developing feedback mechanisms based on spray current measurements.[9,10] Staats et al. sought to account for sudden interruptions of the spray due to emitter clogging, air bubbles, or changes in the eluent composition by adjusting the distance between the emitter and the MS inlet in response to changes in spray current.[9] Gapeev et al. independently built a feedback circuit very similar to the one we described[11] and used it to maintain the electrospray current at a certain level by adjusting the applied voltage.[10] Both techniques disregarded the potential for electrospray switching between operating regimes.

The present report provides insights into the electrospray operation during LC-MS analyses. It is shown that changes in eluent composition during a gradient RPLC analysis are reflected by shifting electrospray characteristic curves. A slow drift of the current generated by an electrospray operated at constant voltage is also demonstrated between LC runs. Two approaches to control the applied voltage through feedback from spray current measurements are discussed.

EXPERIMENTAL SECTION

Sample Preparation

Acetic acid (HOAc), trifluoroacetic acid (TFA) and acetonitrile were purchased from Sigma-Aldrich (St. Louis, MO), and water was purified using a Barnstead Nanopure Infinity system (Dubuque, IA). Solvents A and B consisted of 0.2% HOAc + 0.05% TFA in water and 0.1% TFA in 90:10 acetonitrile:water, respectively. The two solvents were degassed before use by vacuum filtration followed by helium sparging for 10 min. Proteolytic digestion of bovine serum albumin (BSA; Pierce Biotechnology, Rockford, IL) was conducted using sequencing grade trypsin (Promega, Madison, WI) according to established procedures.[12] The BSA tryptic digest was diluted to a concentration of 0.1 μg/μL in purified water and the stock solutions were refrigerated for later use.

Reversed-phase liquid chromatography (RPLC)

LC systems similar to that used here have been described in detail previously.[13,14] Briefly, solvents A and B were loaded into a pair of 100-mL Isco 100DM syringe pumps controlled by

a series D controller (Isco, Lincoln, NE). A 2-position 4-port manually operated valve (Valco Instruments Co., Houston, TX) selected one of the solvents to be delivered into a 2.5-mL mobile phase dynamic mixer (fabricated in-house). The samples were injected using a 2-position 6-port valve (Valco Instruments Co., Houston, TX) with a 5-μL loop. The reversed-phase capillary HPLC column was prepared in-house by slurry packing 3-μm Jupiter C18 stationary phase (Phenomenex, Torrence, CA) into a 60-cm-long, 360-μm o.d. × 75-μm i.d. fused silica capillary tubing (Polymicro Technologies Inc., Phoenix, AZ) incorporating a 0.5-μm retaining screen in a 1/16" union (Valco Instruments Co., Houston, TX) custom bored to 75 μm i.d. (Lenox Laser, Glen Arm, MD). When equilibrated at 5000 psi with 100% mobile phase A, the HPLC system delivered a flow of ~20 μL/min, which was split with a 30-cm long, 20 μm i.d. fused silica tubing to provide ~200 nL/min flow through the HPLC column. Following a 60 min column regeneration with solvent A and 30 min sample load time, the solvent selection valve was switched to deliver solvent B into the mixer, thus creating an exponential gradient.

Spray current measurements

A schematic of the instrument setup is presented in Figure 1. The solution eluting from the chromatographic column was delivered through 20-μm-i.d. electrospray emitters prepared by chemically etching fused silica capillaries.[15] High voltage generated by a Bertan 205B-03R (Hicksville, NY) power supply was applied through a previously described ammeter[11] to the stainless steel union holding the emitter. In this configuration the ammeter measures both the current delivered by electrospray and the current leaking to ground through the HPLC system. To minimize the contribution of the current leaking through the LC column on the spray current measurements, the unions at the two ends of the column were maintained at similar potentials. A National Instruments USB-6251 Multifunction Data Acquisition board (Austin, TX) was used to monitor the ammeter output and to remotely control the high voltage power supply.

MS measurements

Mass spectra were collected using a Micromass Q-TOF Ultima mass spectrometer (Waters Corporation, Milford, MA) with the standard interface replaced by an ion funnel interface with a heated capillary inlet. Decon2LS[16] and MultiAlign,[17] open-source programs developed at PNNL and freely available at http://omics.pnl.gov, were used for data deconvolution and alignment, respectively.

RESULTS AND DISCUSSION

The present study uses a constant pressure LC system delivering a flow of ~200 nL/min, which is amenable to high-throughput, automated LC-MS analyses.[18] At this flow rate, the electrospray characteristic curve (see Figure 1A in reference [5]) can be divided in three sections, each approximating an ohmic response to the applied voltage. At relatively low voltages the liquid wets the outer wall of the emitter; the current increases and the wetted area decreases with increasing applied voltage. The slope decreases slightly when the liquid anchors to the emitter rim; this point will be referred to as the 'anchoring point'. The second section of the curve resembles the pulsating regime observed at lower flow rates but does not have the same self-regulating character. A corona discharge most likely contributes to the current at larger applied voltages,[19] when another change of slope is visible in the characteristic curve; the corresponding point will be referred to as the 'discharge point'. The cone-jet regime could not be established in these experimental conditions. The emitter length and/or the distance to the MS inlet do change the onset voltage of the characteristic curve, but not its appearance.

The appearance of the characteristic curve can be significantly altered by emitter aging - an unavoidable process accompanied by visual and operational clues.[20,21] The walls of fused silica emitters - initially transparent - turn translucent; sometimes residue deposits become

visible. Geromanos et al noticed cavitation and/or cracking of the emitters operated at excessive field strengths.[22] Emitter aging is generally a slow process (days), but can be accelerated significantly (hours) by operation at voltages above the discharge point. Electrospray operation at voltages below the anchoring point can also promote the deposition of residue on the emitter outer wall; however, the emitter aging kinetics seems to be less affected. These physical and/or chemical processes eventually change the wetting properties of the emitter; the liquid maintains the contact with the outer emitter wall even at voltages above the anchoring point, swinging the electrospray to an alternative path in the parameter space. The new path is characterized by poorer reproducibility and noisier current measurements (not shown) due to more erratic fluid dynamics at the tip of a wetted emitter. During this study we tried to prolong the emitter lifetime by avoiding the electrospray operation at voltages above the discharge point. With a single exception (see Figure 2), we also maintained the voltage above the anchoring point.

The characteristic curves obtained for a blank RPLC run, shown in Figure 2 in a color-coded representation, form a gradient map. A base-peak chromatogram, collected at constant voltage, is also provided to illustrate the gradient region of analytical interest. The voltage was scanned in steps of 10 V over a 300 V range above the value generating a threshold spray current, which was set at 30 nA to ensure uninterrupted electrospray operation. During the first 100 minutes of the gradient delivered by the constant pressure LC system, the flow rate increases from ~200 to ~250 nL/min due to decreasing eluent viscosity. The gradient map for an LC system operated at constant flow (~200 nL/min) is expected to be slightly different than that in Figure 2. The spray current would be similar at the beginning of the gradient, but would shift to ~10% smaller values at the end of the analysis. The onset voltages are expected to be insignificantly shifted toward lower values; however, the discharge voltages are somewhat smaller at 200 than at 250 nL/min.[5] Along with an expected slight decrease in ion utilization efficiency, the increased flow rate is expected to improve the robustness of the constant pressure system.

During the time required for the liquid to travel from the mixer to the emitter tip (~15 min) no change in the characteristic curves was observed. A significant drop in the threshold voltage (from 1080 V to 870 V) is readily visible after 100 minutes. This is related to the decreasing surface tension of the eluent as the concentration of the organic component increases. A voltage set 300 V above the threshold generated ~175 nA at the beginning of the gradient and only ~135 nA at the end of the analysis. The decrease of the characteristic curve slope is due to the smaller eluent conductivity. Several minutes after the beginning of the gradient reached the emitter tip, the characteristic curves deviated from the theoretical shape discussed above. The linear dependence between the spray current and the applied voltage was disrupted by the electrospray switching to a multi-jet (rim emission) regime at the top of the applied voltage domain. This regime change produced the yellow peninsula (current ~135 nA) in the gradient map.

Given the changing eluent properties during the LC gradient, it is clear that operating at constant voltage can be problematic. For example, a voltage that delivers abundant current at the beginning of the gradient could later transition to the corona discharge regime. Another scenario could follow the horizontal line corresponding to an applied voltage of ~1275 V, which ensured a current of ~135 nA at the beginning of the gradient. The current would initially increase as the gradient reaches the emitter tip, then decrease due to the electrospray regime shift, and then increase again with increasing content of organic solvent in the eluent. Due to decreasing eluent conductivity, the current would finally decrease by the end of the gradient. Performing the analysis at a voltage that ensures a current less than 135 nA at the end of the gradient (close to 1150 V in this case) seems to be the safest choice. A voltage above the anchoring point at the beginning of the gradient that remains below the corona discharge point

at the end of the gradient would be ideal for RPLC-MS analyses conducted with constant electrospray voltage.

Gradient maps measured at increasing/decreasing emitter-MS inlet distance show voltage shifts to larger/smaller values. Similarly, shorter/longer emitters shift the voltage range to smaller/larger values (not shown). These conditions were maintained during each set of measurements presented (see Figures 3 and 5); however, a new emitter was used for each set of measurements. It is thus likely that the emitters did not have exactly the same length and/or were positioned at slightly different distance from the MS inlet. Consequently, voltage values are strictly comparable only within the same set of measurements, and voltage offsets between sets of measurements are not surprising. The current delivered by the electrospray is a better indicator of the electric field established at the emitter tip, and therefore a better metric to compare different sets of measurements.

Figure 3A presents the base peak ion chromatogram and the spray current measured during an RPLC-MS analysis performed with the electrospray voltage set at 1250 V. The voltage was selected to maintain a spray current lower than 140 nA throughout the gradient. In terms of current generated by the electrospray, these operating conditions would be equivalent to an applied voltage of ~1200 V in Figure 2. The first 60 min of the spray current trace correspond to the column regeneration phase. The arrow marks the sample injection time; the introduction of the sample loop into the circuit affected the leakage current and led to a slightly smaller spray current. The spray current decreased significantly when the solvent from the sample injection loop reached the emitter (~13 minutes later) due to the low solution conductivity. The gradient was initiated at time 0.

Figure 3B shows spray current traces corresponding to four consecutive RPLC-MS analyses performed as described above. Run-to-run variations are visible in this representation, especially for the black trace. We suspect that accumulation of residue on the emitter, which changes the rim geometry and alters the electric field driving the electrospray, is responsible for this drift.

The spray current measurements can be used as feedback to actively maintain the electrospray between the anchoring and the corona discharge points. The corresponding section of the characteristic curve is fairly linear and can be characterized by two coefficients: the slope and the threshold voltage (V_t). These parameters can be calculated by linear regression at any point of the gradient by changing the voltage within a limited range and measuring the corresponding current.

Considering the change in slope at the anchoring point, it is clear that no theoretical significance can be associated to V_t; the practical threshold voltage ensuring the delivery of minimum current by the electrospray is always larger than V_t calculated as described above. The voltage range scanned to collect the data necessary to calculate V_t should be as small as possible to minimize spray current variation that may affect the MS signal. Also, the voltage should be considerably larger than V_t to maintain a reasonable spray current throughout the analysis. Consequently, the extrapolation used to calculate V_t is prone to relatively large errors. However, based on V_t values calculated along the gradient, the applied voltage may be adjusted to maintain the electrospray at equivalent points on the continuously shifting characteristic curves. For example, Figure 4 summarizes the results of an LC-MS run using this feedback algorithm. During this experiment, V_t values were calculated by scanning the voltage in 10 V steps within a 50 V range and the limits of the voltage range were continuously adjusted to maintain the electrospray at least 400 V above V_t.

The voltage decreased from an average of ~1250 V at the beginning of the gradient to an average of ~1000 V at the end of the gradient. Decreasing eluent conductivity led to the spray current declining from an average of ~120 nA to ~80 nA during the analysis. The voltages generating similar currents in Figure 2 were ~1230V and ~1010 V, respectively. This approach leads to relatively large spray current fluctuations, which could be minimized if the determination of new V_t values would be triggered only by significant changes in the spray current or regular time intervals.

The feedback algorithm easiest to implement adjusts the applied voltage to maintain a given spray current. In 1972, Evans and Hendricks built a feedback circuit that regulated the voltage to avoid spontaneous changes in the emission of a liquid metal ion source.[23] Gapeev et al. implemented a similar approach using a proportional-integral-derivative (PID) algorithm,[10] but did not provide any guidance on selecting the spray current level to be maintained. The results presented in this report suggest a linear behavior of the spray current as a function of the applied voltage for our particular experimental conditions. This system should be regulated effectively by a PID algorithm; however, the electrospray characteristic curves are not always linear.[5,24] Even if the assumption of linearity were correct, air bubbles - which are common in LC systems - induce significant spray current drops, which would lead to large voltage overshoots.

Figure 2 suggests that spray currents as high as ~135 nA could be safely maintained throughout the analysis; different solvent combinations or flow rates would require a re-evaluation of this value. Figure 5A summarizes the results of a typical RPLC-MS analysis. The voltage was continuously adjusted to maintain the current at a conservative level of 120 nA throughout the experiment. As in Figure 3A, the first 60 min of the spray current trace correspond to column regeneration. Immediately after sample injection (marked by an arrow), the voltage increased to compensate for the small current drop, after which it was maintained constant while the low-conductivity sample solvent eluted. The gradient was also initiated at time 0.

Figure 5B presents the voltage applied during four consecutive RPLC-MS runs. In good agreement with expectations from Figure 2 (a voltage drop from 1230 V to 1130 V), the voltage dropped ~100 V by the end of the gradient (from 1160 V to 1060 V). This voltage drop was smaller than observed with the previous algorithm (~250 V) and may seem minor when compared to an applied voltage of ~1200 V; however, the voltage drop is significant in comparison with the voltage range that affords the electrospray operation between the anchoring and the corona discharge points.

To maintain a current of 120 nA, the voltage increased slightly at the end of the gradient, compensating for the lower eluent conductivity. There was no major difference between the voltage traces during the first two runs, but the voltage increased ~30 V to generate the same current during the last two runs. As in the case of the experiments performed at constant voltage, we suspect that microscopic deposits on the emitter modified its rim structure, affecting the electric field at its tip. Running the same set of measurements at constant voltage would result in slightly lower spray currents during the last two runs than during the first two runs.

There is a significant difference between the voltage values (1230 V and 1160 V) that ensured the generation of similar spray current (120 nA) in Figures 2 and 5; this may be related to different emitter length and/or positioning relative to the MS inlet. Assuming that operation at constant voltage was desirable for the experiments in Figure 5, a voltage of 1230 V would be selected using Figure 2 as benchmark and without any hint of this voltage shift. The resulting electric field would draw ~155 nA at the beginning of the analysis, which would be appropriate at the start of the gradient but excessive at the end.

To evaluate the effect of the small run-to-run spray current drift observed when the electrospray was operated at constant voltage (Figure 3B), we considered the species detected in all four measurements to calculate the reproducibility of the corresponding analytical signal. The coefficient of variance was slightly lower than 30%, a level roughly equivalent to that found for label-free quantitation in LC-MS studies.[25,26] The measurements with feedback control (Figure 5B) resulted in similar coefficient of variance. It may seem surprising that compensating for the spray current drift did not improve the reproducibility of the data. We can interpret this observation in the light of our recent results[11] showing that ionization and transmission efficiencies balance fortuitously for electrosprays operated at relatively large flow rates, offering greater robustness at the cost of smaller ion utilization efficiency.

CONCLUSIONS

Spray current measurements can be used to monitor the electrospray operation throughout gradient LC-MS measurements. Even if not used as feedback for voltage control, they can still provide a reliable quality control mechanism and important information regarding electrospray operation by diagnosing emitter clogging, the presence of air bubbles in the eluent, and emitter aging. Based on gradient maps, the electrospray voltage can be rationally selected to ensure optimal operation throughout the analysis. We expect that the small current drift observed during the four LC-MS runs at constant voltage (Figure 3B) becomes more significant with emitter aging and would eventually alter the quality of the data collected at constant electrospray voltage. We are in the process of integrating the spray current monitoring and voltage selection/regulation approaches in our automated LC-MS systems.[18] This will enable longer term studies of electrospray behavior that will further clarify the effect of voltage regulation on the LC-MS data reproducibility.

We have shown that our particular experimental conditions afford the electrospray operation at a constant but rigorously selected voltage with no negative impact on the reproducibility of the MS signal. However, these results should not be interpreted to suggest that an electrospray can be operated at constant voltage without unfavorable consequences throughout any LC-MS experiment. Selection of the electrospray voltage for the vast majority of LC-MS analyses is less rigorous than presented here; the voltage optimization at the beginning of the analysis often results in poor electrospray operation at the end of the gradient. Changing electrospray operating regimes and/or faster emitter aging due to wetting/corona discharges are expected to induce larger run-to-run spray current fluctuations, which could affect the analyte ionization and the MS signal more significantly.

This study is relevant for experiments in which the electrospray characteristic curves are virtually linear. Experimental conditions that bring more definition to the shape of the characteristic curves (different solvent systems, solvents of much lower conductivity, lower flow rates, flow split through multi-emitter arrays[27]) could benefit significantly from more sophisticated voltage control algorithms.

ACKNOWLEDGMENTS

We thank Dr. Yehia M. Ibrahim and Heather M. Mottaz for providing BSA samples, Dr. Eric A. Livesay, Rui Zhao, Daniel Orton, and Dr. Kostantinos Petritis for assistance with LC-MS operation, Dr. Christina M. Sorensen, Dr. Tyler Heibeck, Dr. Vlad A. Petyuk, and Dr. Ashoka D. Polpitiya for sharing their experience with LC-MS data analysis procedures. This research was supported by the NIH National Center for Research Resources (RR018522). Experimental portions were performed in the Environmental Molecular Sciences Laboratory, a DOE national scientific user facility located at the PNNL in Richland, Washington. PNNL is a multiprogram national laboratory operated by Battelle for the DOE under Contract DE-AC05-76RLO 1830.

REFERENCES

1. Aleksandrov ML, Gall LN, Krasnov VN, Nikolaev VI, Pavlenko VA, Shkurov VA, Baram GI, Gracher MA, Knorre VD, Kusner YS. On the working characteristics of an ion source with eletrohydrodynamic introduction of liquids into the mass spectrometer. Bioorg. Khim 1984;10:710–712.
2. Whitehouse CM, Dreyer RN, Yamashita M, Fenn JB. Electrospray interface for liquid chromatographs and mass spectrometers. Anal. Chem 1985;57:675–679. [PubMed: 2581476]
3. Aebersold R, Mann M. Mass spectrometry-based proteomics. Nature 2003;422:198–207. [PubMed: 12634793]
4. Domon B, Aebersold R. Review - Mass spectrometry and protein analysis. Science 2006;312:212–217. [PubMed: 16614208]
5. Marginean I, Kelly RT, Page JS, Tang K, Smith RD. Electrospray characteristic curves: In pursuit of improved performance in the nanoflow regime. Anal. Chem 2007;79:8030–8036. [PubMed: 17896826]
6. Jackson GS, Enke CG. Electrical equivalence of electrospray ionization with conducting and nonconducting needles. Anal. Chem 1999;71:3777–3784. [PubMed: 10489527]
7. Ramanathan R, Zhong R, Blumenkrantz N, Chowdhury SK, Alton KB. Response normalized liquid chromatography nanospray ionization mass Spectrometry. J. Am. Soc. Mass Spectrom 2007;18:1891–1899. [PubMed: 17766144]
8. Valaskovic GA, Murphy JP, Lee MS. Automated orthogonal control system for electrospray ionization. J. Am. Soc. Mass Spectrom 2004;15:1201–1215. [PubMed: 15276167]
9. Staats, SLT.; Fogiel, AJ.; Suna, A. Active spray control with electric field optimization for online NanoLC with polymeric spray tips; 56th ASMS Conference on Mass Spectrometry; Denver, CO. 2008; Jun 1-5.
10. Gapeev, A.; Berton, A.; Fabris, D. Current-controlled nanospray for the analysis of less than ideal samples; 56th ASMS Conference on Mass Spectrometry; Denver, CO. 2008; Jun 1-5.
11. Marginean I, Kelly RT, Prior DC, LaMarche BL, Tang K, Smith RD. Analytical Characterization of the Electrospray Ion Source in the Nanoflow Regime. Anal. Chem 2008;80:6573–6579. [PubMed: 18661954]
12. Kinter, MM.; Sherman, NE. Protein Sequencing and Identification Using Tandem Mass Spectrometry. Wiley-Interscience; New York: 2000.
13. Shen YF, Tolic N, Zhao R, Pasa-Tolic L, Li LJ, Berger SJ, Harkewicz R, Anderson GA, Belov ME, Smith RD. High-throughput proteomics using high efficiency multiple-capillary liquid chromatography with on-line high-performance ESI FTICR mass spectrometry. Anal. Chem 2001;73:3011–3021. [PubMed: 11467548]
14. Shen YF, Zhao R, Belov ME, Conrads TP, Anderson GA, Tang KQ, Pasa-Tolic L, Veenstra TD, Lipton MS, Udseth HR, Smith RD. Packed capillary reversed-phase liquid chromatography with high-performance electrospray ionization Fourier transform ion cyclotron resonance mass spectrometry for proteomics. Anal. Chem 2001;73:1766–1775. [PubMed: 11338590]
15. Kelly RT, Page JS, Luo QZ, Moore RJ, Orton DJ, Tang KQ, Smith RD. Chemically etched open tubular and monolithic emitters for nanoelectrospray ionization mass spectrometry. Anal. Chem 2006;78:7796–7801. [PubMed: 17105173]
16. Jaitly N, Mayampurath A, Littlefield K, Adkins JN, Anderson GA, Smith RD. Decon2LS: An open-source software package for automated processing and visualization of high resolution mass spectrometry data. BMC Bioinformatics. 2008submitted
17. Jaitly N, Monroe ME, Petyuk VA, Clauss TRW, Adkins JN, Smith RD. Robust algorithm for alignment of liquid chromatography-mass spectrometry analyses in an accurate mass and time tag data analysis pipeline. Anal. Chem 2006;78:7397–7409. [PubMed: 17073405]
18. Livesay EA, Tang KQ, Taylor BK, Buschbach MA, Hopkins DF, LaMarche BL, Zhao R, Shen YF, Orton DJ, Moore RJ, Kelly RT, Udseth HR, Smith RD. Fully automated four-column capillary LC-MS system for maximizing throughput in proteomic analyses. Anal. Chem 2008;80:294–302. [PubMed: 18044960]

19. Marginean I, Kelly RT, Prior DC, LaMarche BL, Tang KQ, Smith RD. Analytical characterization of the electrospray ion source in the nanoflow regime. Anal. Chem 2008;80:6573–6579. [PubMed: 18661954]

20. Nilsson S, Svedberg M, Pettersson J, Bjorefors F, Markides K, Nyholm L. Evaluations of the stability of sheathless electrospray ionization mass spectrometry emitters using electrochemical techniques. Anal. Chem 2001;73:4607–4616. [PubMed: 11605837]

21. Chen ML, Cook KD. Oxidation artifacts in the electrospray mass spectrometry of A beta peptide. Anal. Chem 2007;79:2031–2036. [PubMed: 17249640]

22. Geromanos S, Freckleton G, Tempst P. Tuning of an electrospray ionization source for maximum peptide-ion transmission into a mass spectrometer. Anal. Chem 2000;72:777–790. [PubMed: 10701263]

23. Evans CA, Hendricks CD. Electrohydrodynamic ion-source for mass-spectrometry of liquids. Rev. Sci. Instrum 1972;43:1527–1530.

24. Chen DR, Pui DYH, Kaufman SL. Electrospraying of conducting liquids for monodisperse aerosol generation in the 4 nm to 1.8 um diameter range. J. Aerosol. Sci 1995;26:963–977.

25. Old WM, Meyer-Arendt K, Aveline-Wolf L, Pierce KG, Mendoza A, Sevinsky JR, Resing KA, Ahn NG. Comparison of label-free methods for quantifying human proteins by shotgun proteomics. Mol. Cell. Proteomics 2005;4:1487–1502. [PubMed: 15979981]

26. Ono M, Shitashige M, Honda K, Isobe T, Kuwabara H, Matsuzuki H, Hirohashi S, Yamada T. Label-free quantitative proteomics using large peptide data sets generated by nanoflow liquid chromatography and mass spectrometry. Mol. Cell. Proteomics 2006;5:1338–1347. [PubMed: 16552026]

27. Kelly RT, Page JS, Marginean I, Tang KQ, Smith RD. Nanoelectrospray emitter arrays providing interemitter electric field uniformity. Anal. Chem 2008;80:5660–5665. [PubMed: 18553942]

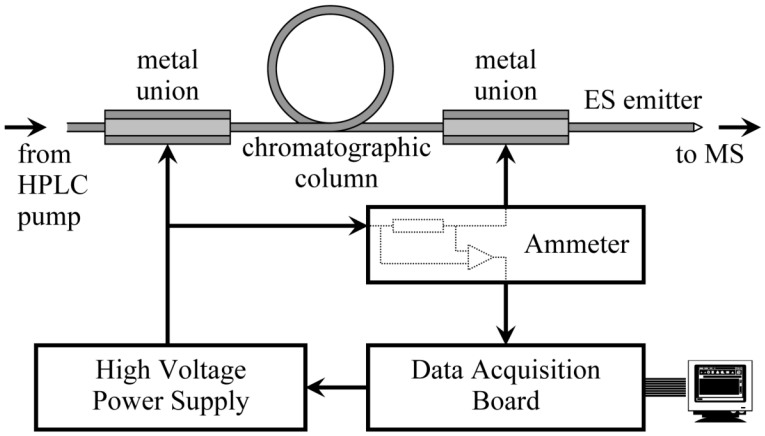

Figure 1.
Instrumental setup. See reference [11] for a detailed description of the ammeter circuit.

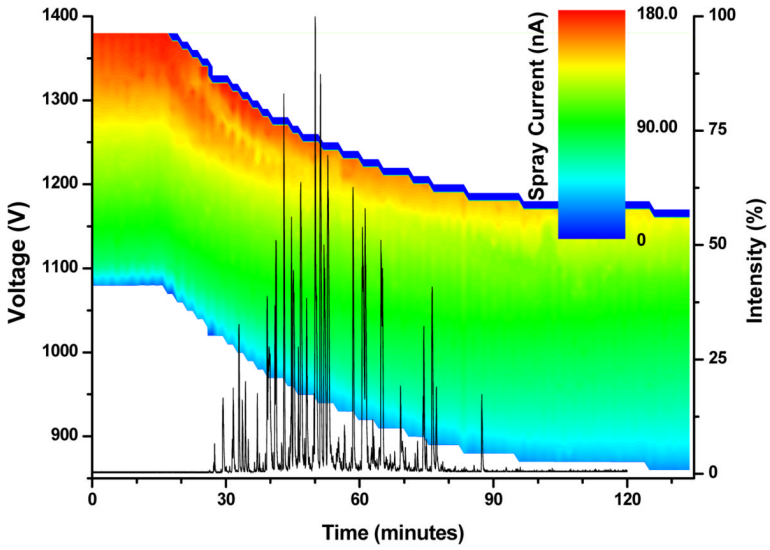

Figure 2.
Electrospray characteristic curves measured during a gradient LC-MS dry run superimposed on a base peak ion chromatogram to illustrate the domain of analytical interest.

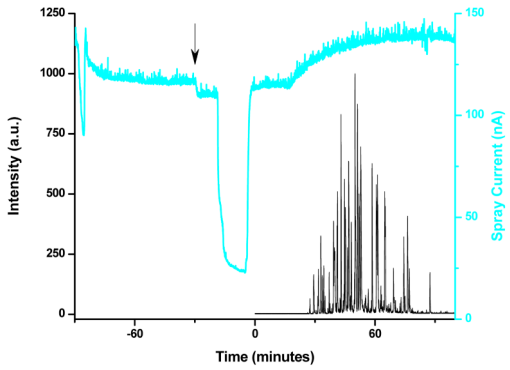

A

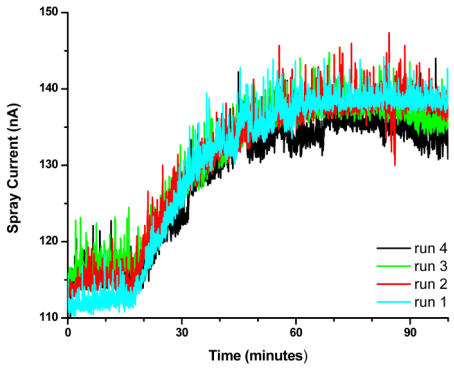

B

Figure 3.

Base peak ion chromatogram and spray current for LC-MS analysis performed with constant voltage (1250 V) applied to electrospray (A). Spray current traces for four consecutive LC-MS analyses (B).

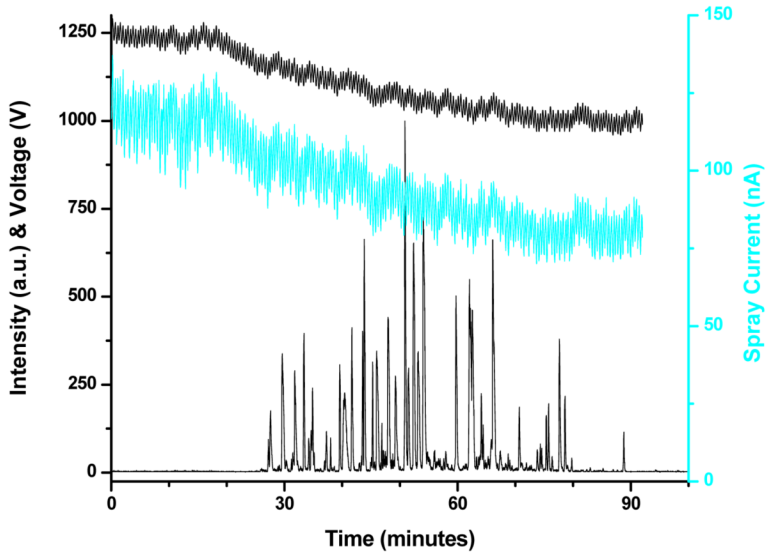

Figure 4.
LC-MS analysis performed using feedback from spray current measurements to control the voltage with minimal a priori knowledge about the LC gradient (see text for details).

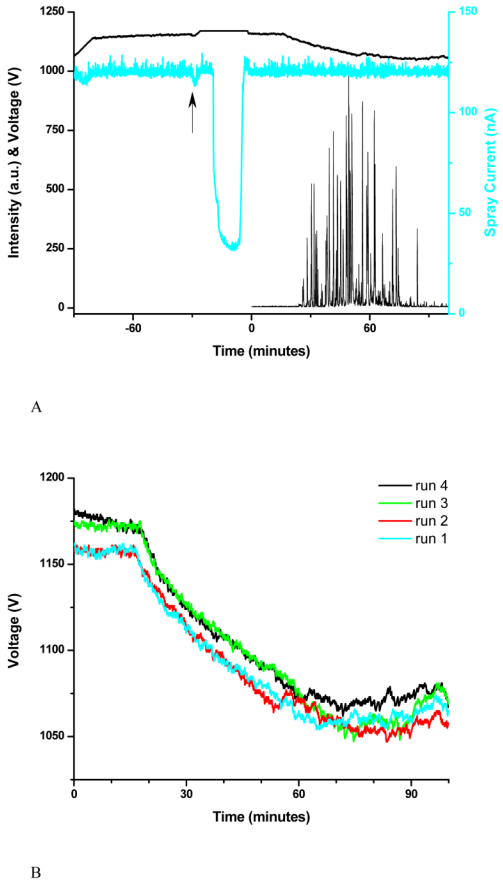

Figure 5.
Base peak ion chromatogram, applied voltage and spray current for LC-MS analysis performed with feedback control of the applied voltage (A). Applied voltage traces for four consecutive LC-MS analyses (B).